

# Estimating the Impulse Response of Buried Objects from Ground Penetrating Radar Signals

Fedde van der Lijn<sup>a</sup>, Friedrich Roth<sup>a</sup>, Michel Verhaegen<sup>b\*</sup>

<sup>a</sup> International Research Centre for Telecommunications-transmission and Radar (IRCTR)

<sup>b</sup> Control Systems Engineering Group

Faculty of Information Technology and Systems, Delft University of Technology,  
Mekelweg 4, 2600 GA Delft, The Netherlands

## ABSTRACT

This paper presents a novel deconvolution algorithm designed to estimate the impulse response of buried objects based on ground penetrating radar (GPR) signals. The impulse response is a rich source of information about the buried object and therefore very useful for intelligent signal processing of GPR data. For example, it can be used in a target classification scheme to reduce the false alarm rate in demining operations. Estimating the target impulse response from the incident and scattered radar signals is a basic deconvolution problem. However, noise sensitivity and ground dispersion prevent the use of simple deconvolution methods like linear least squares deconvolution. Instead, a new deconvolution algorithm has been developed that computes estimates adhering to a physical impulse response model and that can be characterized by a limited number of parameters. It is shown that the new algorithm is robust with respect to noise and that it can deal with ground dispersion. The general performance of the algorithm has been tested on data generated by finite-difference time-domain (FDTD) simulations. The results demonstrate that the algorithm can distinguish between different dielectric and metal targets, making it very suitable for use in a classification scheme. Moreover, since the estimated impulse responses have physical meaning they can be related to target characteristics such as size and material properties. A direct application of this is the estimation of the permittivity of a dielectric target from its impulse response and that of a calibration target.

**Keywords:** ground penetrating radar, signal processing, landmine identification, target impulse response, deconvolution, subset selection, noise sensitivity, ground dispersion.

## 1. INTRODUCTION

The metal detector is currently the most widely used type of detector in demining operations. However, it has a serious shortcoming: its false alarm rate is very high. Therefore, research is done on other detectors that can act as an addition or alternative to the metal detector. One of these possible additions is the ground penetrating radar (GPR).

The most important advantage of using GPR in mine detection is the extraction of target information. This information can be used in intelligent signal processing schemes to reduce the false alarm rate. An example of GPR signal processing is target classification based on the target impulse response. The impulse response is a rich source of target characteristics such as size, material composition and depth. These characteristics can be used to distinguish minelike targets from clutter or harmless buried objects.

Obtaining the target impulse response from GPR signals is a deconvolution problem. However, using simple deconvolution methods like the linear least squares deconvolution can prove difficult because of noise sensitivity and ground dispersion. Noise sensitivity is a common problem when deconvolving signals from badly conditioned systems. It could be solved by using robust deconvolution methods like ridge regression<sup>1</sup> or by increasing the bandwidth of the radar pulse. But even if the noise sensitivity is reduced in these ways, ground dispersion will remain a problem. Ground

---

\* Further author information:

F.v.d.L.: E-mail: [feddevanderlijn@myrealbox.com](mailto:feddevanderlijn@myrealbox.com)

F.R.: E-mail: [f.roth@irctr.tudelft.nl](mailto:f.roth@irctr.tudelft.nl), Phone: +31/15/278 3815

M.V.: E-mail: [m.h.g.verhaegen@its.tudelft.nl](mailto:m.h.g.verhaegen@its.tudelft.nl), Phone: +31/15/278 5204

attenuation is generally frequency dependent. This causes the soil to act as a low pass filter, smearing the radar pulse to an unknown degree. Therefore the signal is not only altered by the target, but also by the ground. These two effects cannot be easily separated.

Much literature exists on obtaining the impulse response of a badly conditioned system. However, very little is known on obtaining the impulse response from smeared GPR signals. Scheers<sup>2</sup> briefly discusses the subject, but he is unable to solve the dispersion problem.

To solve both the noise sensitivity and the dispersion problem, an algorithm has been developed that uses a priori information on the form of the impulse response of minelike targets. This information is taken from a physical model for the impulse response of minelike targets developed by Roth et al<sup>3</sup>. Using the Born scattering approximation, Roth et al derived an expression for the combination of impulse response coefficients that corresponds to contrasts in dielectric permittivity. The deconvolution algorithm described in this paper searches for an impulse response consisting of these combinations of coefficients.

The paper is organized as follows. In section 2, two physical impulse response models from the literature including the one developed by Roth et al are reviewed. The two models are illustrated using a dielectric and a metal disk as example targets. Section 3 describes the new deconvolution algorithm, which is based on these physical impulse response models, and its robustness to ground dispersion is illustrated by a numeric example. Section 4 discusses the algorithm's ability to distinguish between different targets. This ability has been tested by estimating the impulse responses of different targets using signals generated by finite-difference time-domain (FDTD) simulations. Conclusions are given in section 5.

## 2. THE IMPULSE RESPONSE OF MINELIKE TARGETS

The new deconvolution algorithm is based on approximate physical models for the far-field axial impulse response of a circular homogeneous dielectric or metal disk embedded in a lossless soil. The radar wave illuminating the disk is assumed to be plane. For the dielectric disk, the impulse response can be approximated by<sup>3</sup>

$$g(t) = -\frac{\mu_0 v}{4\sqrt{\pi}} A \Delta \varepsilon \left[ \delta'(t) - \Gamma \delta'(t - 2l/v_{eff}) \right]. \quad (1)$$

The impulse response of the metal disk according to the physical optics scattering approximation is given by<sup>4</sup>

$$g(t) = -\frac{1}{v\sqrt{\pi}} A \delta'(t). \quad (2)$$

In these equations  $A$  represents the cross-section of the disk,  $v$  is the wave velocity in the soil and  $\delta'(t)$  is the derivative of the delta function. This corresponds to a differential operator. In equation (1),  $\mu_0$  is the magnetic permeability of vacuum,  $\Delta \varepsilon$  represents the permittivity contrast between the target and the soil,  $l$  is the thickness of the disk,  $v_{eff}$  is the effective velocity of the wave traveling through and along the surface of the disk and  $\Gamma$  is a scaling factor accounting for the transmission losses at the top of the target. Equations (1) and (2) imply that a disk differentiates the waveform of the incident plane wave.

As a first example, the impulse response of a target comparable to a PMA-3 type mine is calculated. This target is a truncated circular cylinder with a thickness of 4 cm and a diameter of 10 cm. It is filled with a dielectric material having a relative dielectric permittivity of 2.8, which is representative for plastics and explosives. The target is embedded in a homogeneous soil having a relative dielectric permittivity of 4. Values for  $\Gamma$  and  $v_{eff}$  were determined by comparing the model of equation (1) to FDTD simulations of the target response.<sup>3</sup> It was found that for this target  $\Gamma$  is equal to 0.7 and  $v_{eff}$  is equal to the average of the wave velocity in the soil and the wave velocity in the target.

The resulting impulse response of this target is shown in figure 1. The two discrete differential operators in the figure are the result of the dielectric permittivity contrast between the target and the surrounding medium. The first operator corresponds to backscatter from the top of the landmine whereas the second relates to backscatter from the bottom of the landmine.

The impulse response contains important information on the target and the soil. Equation (1) shows that the magnitude of the first differential operator depends on the target cross-section and the permittivity contrast between the target and the soil. Furthermore, the distance between the differential operators is a measure of the thickness of the target and its material composition.

Figure 2 shows the impulse response of a metal disk. The target is modeled as a perfect electrical conductor having the same dimensions as the previous example target. The impulse response of this target only consists of a single differential operator since metal is a perfect reflector. This is also the reason why the differential operator for the metal disk has a larger magnitude than the differential operators of the impulse response of the dielectric target.

### 3. SUBSET SELECTION DECONVOLUTION ALGORITHM

For discrete time steps, the scattered signal  $\mathbf{y}$  satisfies

$$\mathbf{y} = \mathbf{X}\mathbf{g} , \quad (3)$$

where  $\mathbf{y} \in \mathfrak{R}^M$ ,  $\mathbf{g} \in \mathfrak{R}^N$  and  $\mathbf{X} \in \mathfrak{R}^{M \times N}$ . The vector  $\mathbf{g}$  represents the target impulse response.  $\mathbf{X}$  is the convolution matrix constructed from the incident signal  $\mathbf{x} = [x(0) \ x(1) \ \dots \ x(P)]^T$ , which is the time function of the wave illuminating the target.  $\mathbf{X}$  is defined as

$$\mathbf{X} = [\mathbf{x}_1 \ \mathbf{x}_2 \ \dots \ \mathbf{x}_N] = \begin{bmatrix} x(0) & 0 & \dots & 0 \\ x(1) & x(0) & \ddots & \vdots \\ \vdots & x(1) & \ddots & 0 \\ x(P) & \vdots & \ddots & x(0) \\ 0 & x(P) & & x(1) \\ \vdots & \ddots & \ddots & \vdots \\ 0 & \dots & 0 & x(P) \end{bmatrix} . \quad (4)$$

Here  $\mathbf{x}_i$  ( $i=1, \dots, N$ ) denote the column vectors of  $\mathbf{X}$ .

The least squares estimate of the target impulse response is found by solving

$$\min_{\mathbf{g}} \|\mathbf{X}\hat{\mathbf{g}} - \mathbf{y}\|_2^2 , \quad (5)$$

which results in an estimated target impulse response  $\hat{\mathbf{g}}$  given by<sup>1</sup>

$$\hat{\mathbf{g}} = (\mathbf{X}^T \mathbf{X})^{-1} \mathbf{X}^T \mathbf{y} . \quad (6)$$

When solving the least squares problem for GPR signals, noise sensitivity will often be a problem. Sampling times used in GPR systems for mine detection are small (e.g. 10 ps) compared to the width of the incident radar pulse (e.g. 1.8 ns). This causes  $\mathbf{X}$  to have a high condition number, making the least squares solution vulnerable to additive signal disturbances.

Moreover, frequency dependent soil properties can cause problems for the standard least squares deconvolution algorithm as illustrated by the following numeric example. Incident and scattered signals were computed on the basis of the signal radiated by an ultra-wideband GPR system developed at the International Research Centre for Telecommunications-transmission and Radar (IRCTR).<sup>5</sup> Filtering of this radar signal by a low-pass filter simulated the smearing effect of soil with frequency dependent attenuation. The low-pass filter is based on the so-called constant Q model.<sup>6</sup> In this example, the filter was designed to describe the propagation through 10 cm of a sandy soil with 5% moisture content ( $\epsilon_r = 4$ ,  $Q^* = 6.0$ ). The filtered radar signal was used as the incident signal  $\mathbf{x}$ . The scattered signal  $\mathbf{y}$  was generated by convolving the incident signal  $\mathbf{x}$  with the target impulse response shown in figure 1. The computed incident and scattered signals were then used as input to the standard least squares deconvolution algorithm, yielding the estimated target impulse response shown in figure 3. The impulse response estimate clearly shows the effect of the soil: the differential operators of the original target impulse response are smeared out, making the target impulse response unrecognizable.

A new deconvolution algorithm has been designed to overcome these problems. Contrary to the standard least squares solution, this new algorithm uses a limited subset of columns of the convolution matrix  $\mathbf{X}$  to approximate the scattered signal  $\mathbf{y}$ . This has the advantage of improving the condition number of  $\mathbf{X}$ , thereby decreasing the noise sensitivity. Furthermore, the algorithm only considers impulse responses that consist of one (metal target) or two (penetrable target) discrete differential operators. The impulse response estimates therefore always adhere to the physical models presented in the previous section.

When a discrete differential operator is applied to the incident signal at time step  $i$ , the resulting signal is equal to the difference between the  $(i - 1)^{\text{th}}$  and  $(i + 1)^{\text{th}}$  column of  $\mathbf{X}$ :

$$\Delta_i \mathbf{x} = \mathbf{x}_{i-1} - \mathbf{x}_{i+1} . \quad (7)$$

For a penetrable target, the new algorithm computes an estimate of the target impulse response by finding optimal locations and magnitudes for two discrete differential operators. This is achieved by solving the following modified least squares problem:

$$\min_{i,j} \left( \min_{\mathbf{h}} \left\| \mathbf{X}_{i,j}^S \mathbf{h} - \mathbf{y} \right\|_2^2 \right) , \quad (8)$$

where  $\mathbf{y} \in \mathfrak{R}^M$ ,  $\mathbf{h} = [h_1 \ h_2]^T \in \mathfrak{R}^2$  and  $\mathbf{X}_{i,j}^S \in \mathfrak{R}^{M \times 2}$ . The matrix  $\mathbf{X}_{i,j}^S$  is defined as

$$\mathbf{X}_{i,j}^S = [\Delta_i \mathbf{x} \quad \Delta_j \mathbf{x}] . \quad (9)$$

For metal targets, the algorithm only needs to find the optimal location and magnitude for one differential operator. The optimization is achieved by solving a modified least squares problem similar to the one formulated for two discrete differential operators, except that the problem dimensions change to  $\mathbf{h} = [h_1] \in \mathfrak{R}$  and  $\mathbf{X}_i^S = [\Delta_i \mathbf{x}] \in \mathfrak{R}^{M \times 1}$ . It should be noted that the subset selection deconvolution algorithm can also easily be extended to allow for more than two discrete differential operators. This might become necessary when dealing with complex targets that exhibit internal structure.

Expression (8) shows a major advantage of the subset selection deconvolution algorithm. The estimated impulse response of a penetrable target can be characterized by four parameters: the locations  $i$  and  $j$  of the differential operators and their magnitudes  $h_1$  and  $h_2$ . The impulse response of a metal target can be described by two parameters. Compare this to the standard least squares estimate that is characterized by  $N$  parameters. The limited number of parameters makes the results of the algorithm easy to use in a classification scheme. Furthermore, the estimated impulse responses have physical meaning and can be related to target characteristics such as size and material composition through equations (1) and (2).

Applying this algorithm to the filtered signals described above yields the estimated impulse response shown in figure 4. The figure shows that this estimate, contrary to the least squares estimate, is not affected by the ground dispersion. In addition, the relative characteristics of the original target impulse response shown in figure 1 are retained. Comparing the estimated against the original target impulse response shows that the distance between the differential operators as well as the ratio of the second operator magnitude over the first operator magnitude, i.e.  $h_2 / h_1$ , are recovered correctly. These relative characteristics are important for target classification.

#### 4. ESTIMATING THE IMPULSE RESPONSE FOR DIFFERENT TARGETS

In the previous section it was shown that the subset selection deconvolution algorithm is robust. It can handle ground dispersion and decreases noise sensitivity. But since it will be used in a target classification scheme, it is also necessary to show that the algorithm is able to distinguish between different targets.

This ability was tested by using pairs of incident and scattered signals for different minelike targets, generated with a 3D FDTD simulation program.<sup>7</sup> The simulations assumed a target embedded in a homogeneous lossless medium. The host medium's relative dielectric permittivity was set equal to 4. The target was illuminated at normal incidence by a linearly polarized plane wave. The time function of the incident plane wave was a Ricker wavelet (2<sup>nd</sup> derivative of a Gaussian pulse) with a peak amplitude frequency of 1.5 GHz. The scattered wave was considered at a location 60 cm above the target. Table 1 lists the different target types used in the test.

The results of applying the subset selection deconvolution algorithm on these targets are summarized in table 2. The results prove that the estimated parameters are proportional to the physical dimensions of the targets. Table 1 shows that the minelike target 1 (PMA-3) and the minelike target 3 (M14) are of equal thickness, while the minelike target 2 is 50% thicker. The estimated distance  $(j-i)$  between the differential operators should exhibit similar ratios since it is proportional to the target thickness. This proves to be the case:  $(j-i)$  is equal for the PMA-3 and the M14. For the minelike target 2 the estimated distance is 45% bigger than that of the PMA-3. Furthermore, equation (1) shows that the magnitude of the first differential operator  $h_1$  should be proportional to the target cross-section. The cross-section of the minelike target 2 is more than twice as big as that of the PMA-3. For the minelike target 2 the magnitude  $h_1$  is indeed 220% of  $h_1$  for the PMA-3. The cross-section of the M14 is 35% of the cross-section of the PMA-3. The magnitude estimates  $h_1$  for these targets show approximately the same ratio. The estimated impulse response of the metal disk is also consistent with the theory:  $h_1$  for this target is much larger than  $h_1$  for a dielectric target since metal is a perfect reflector.

The fact that the estimated target impulse responses adhere to the physical models described by equations (1) and (2) allows for the estimation of the relative permittivity of a dielectric target from its impulse response and the impulse response of a metal disk:

$$\epsilon_{r,\text{target}} = \epsilon_{r,\text{soil}} \left( 1 + 4 \frac{A_{\text{metal disk}} h_{1,\text{target}}}{A_{\text{target}} h_{1,\text{metal disk}}} \right). \quad (10)$$

Applying equation (10) to the estimated impulse responses, yields a relative permittivity of approximately 2.6 for all three dielectric minelike targets, which is close to their true relative permittivity (2.8). This result suggests the interesting possibility to determine the permittivity of a buried target from GPR measurements over the target and a calibration target (metal disk). It is important to note however that there are some limitations to this method. First, the two targets need to be buried at the same depth. Moreover, the cross-section of the target in question is unknown and hence the method relies on assuming a certain value for the cross-section. And finally, the soil dielectric permittivity has to be estimated by fitting hyperbolas present in the GPR data or needs to be measured in the laboratory.

Figure 5 shows the scattered signals obtained from the FDTD simulations and the scattered signals estimated by the subset selection deconvolution algorithm. The figure shows that there is an excellent fit between the two types of scattered signals. This demonstrates that it is possible to accurately reconstruct the FDTD scattered signals using very simple target impulse responses. For example, the scattered signal of the metal disk is well estimated by a target impulse response consisting of only one differential operator. This observation supports the subset selection approach.

## 5. CONCLUSIONS

The results of the previous sections show that the subset selection deconvolution algorithm is well suited to estimate the target impulse response of a buried homogeneous object. It characterizes the target impulse response by a limited number of parameters, making the results easy to use in a classification scheme. Differences in target size are proportionally reflected in these parameters, making it possible for the algorithm to distinguish between different targets. Since the estimated impulse responses adhere to a physical model, they can be used to determine the permittivity of a buried dielectric target.

The algorithm is robust; it is less sensitive to noise than the standard least squares deconvolution. Moreover, it can make accurate estimates of the target impulse response even when the target is buried in dispersive soil. This cannot be achieved with the standard least squares deconvolution.

Future research will focus on the application of the subset selection deconvolution algorithm to real GPR data acquired over a set of well-defined targets including test mines and calibration targets buried at various depths.

## ACKNOWLEDGEMENTS

This research was funded by the Dutch Technology Foundation STW, applied science division of NWO.

## REFERENCES

1. G. Golub and C. Van Loan, *Matrix Computations*, 3<sup>rd</sup> Edition, Johns Hopkins University Press, Baltimore, 1996.
2. B. Scheers, *Ultra-Wideband Ground Penetrating Radar, with Application to the Detection of Anti Personnel Landmines*, PhD Thesis, Royal Military Academy, Brussels, Belgium, 2001.
3. F. Roth, P. van Genderen, M. Verhaegen, "Radar response approximations for buried plastic landmines", *Proc. SPIE 4758*, 9<sup>th</sup> International Conference on Ground Penetrating Radar, April 29-May 2, 2002, Santa Barbara, CA, pp. 246-250, 2002.
4. S. Nag and L. Peters, "Ramp Response Signatures for Dielectric Targets", *Proc. SPIE 3392*, Detection and Remediation Technologies for Mines and Minelike Targets III, April 1998, Orlando, FL, pp. 703-713, 1998.
5. P. van Genderen, G.P. Hermans, I. Morrow, B. Sai, A. Yarovoy, N.V. Budko, S. L. T. J. van der Laan and J. van Heijenoort, *Video impulse radar for landmine detection*, IRCTR, Delft University of Technology, The Netherlands, Tech. Rep. S-008-00, 1999.
6. F. van der Lijn, *Deconvolution of the impulse response of mine-like targets using ground penetrating radar signals*, MSc Thesis, University of Twente, The Netherlands, 2002.
7. G. Mur, *FDTD3D: The C++ Finite-Difference Code for Electromagnetic Fields in Three Dimensions and Time*, IRCTR and Laboratory of Electromagnetic Research, Delft University of Technology, The Netherlands, 2001.

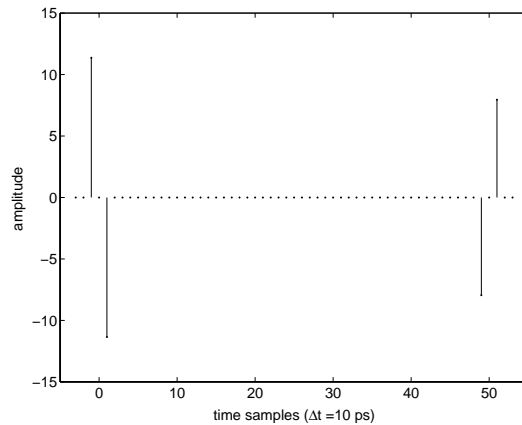


Figure 1: Impulse response of the PMA-3-like target according to the physical impulse response model of equation (1).

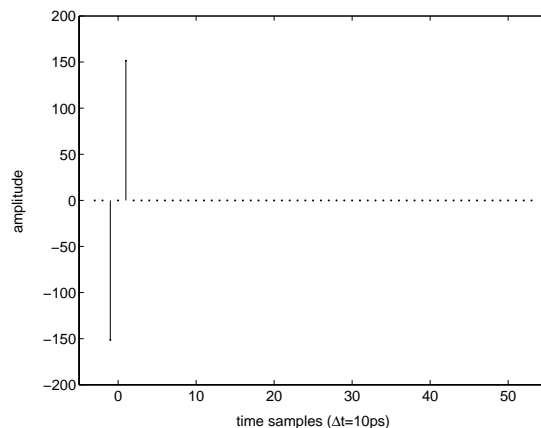


Figure 2: Impulse response of the metal disk according to the physical impulse response model of equation (2).

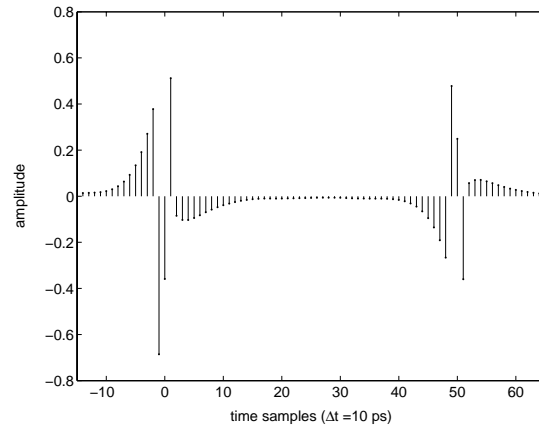


Figure 3: Impulse response estimate of the PMA-3-like target in a dispersive medium computed with the standard least squares deconvolution algorithm.

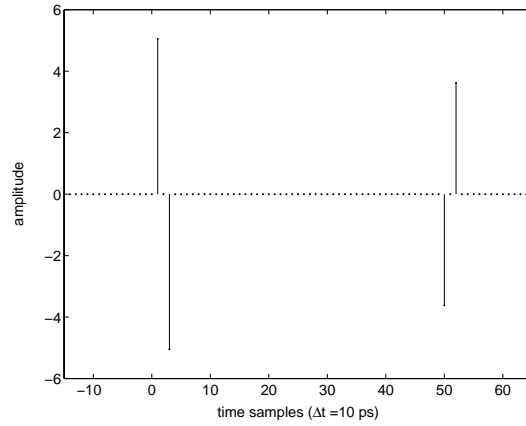


Figure 4: Impulse response estimate of the PMA-3-like target in a dispersive medium computed with the subset selection deconvolution algorithm.

Table 1: Description of the targets used to test the algorithm's ability to distinguish between different targets.

Target	Shape	Radius[cm]	Cross-section [cm <sup>2</sup> ]	Thickness [cm]	Material
minelike target 1 (PMA-3)	TCC*	5.0	79	4.0	dielectric, $\epsilon_r = 2.8$
minelike target 2	TCC	7.5	177	6.0	dielectric, $\epsilon_r = 2.8$
minelike target 3 (M14)	TCC	3.0	28	4.0	dielectric, $\epsilon_r = 2.8$
metal disk	TCC	5.0	79	4.0	PEC**

\* Truncated circular cylinder

\*\* Perfect electrical conductor

Table 2: Results of the subset selection deconvolution algorithm for the targets listed in table 1. Note that the huge differences between the operator magnitudes in this table and those of the example target impulse responses in figures 1 and 2 are a result of geometrical spreading, which is not accounted for in equations (1) and (2). Furthermore, a larger time sampling interval is considered (14 ps instead of 10 ps).

Target	$h_1$	$h_2$	$(j-i)$	$ h_2/h_1 $
minelike target 1 (PMA-3)	0.043	-0.029	33	0.67
minelike target 2	0.095	-0.063	48	0.66
minelike target 3 (M14)	0.015	-0.008	33	0.54
metal disk	-0.482	-	-	-

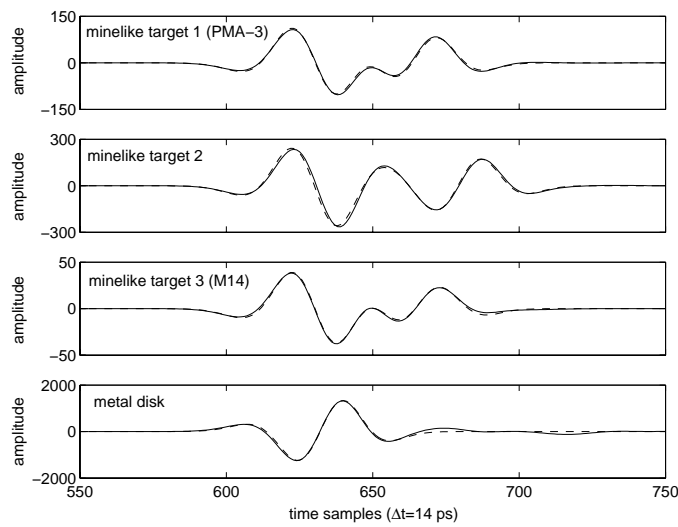


Figure 5: Comparison of the scattered signals estimated by the subset selection deconvolution algorithm (dashed lines) against the scattered signals obtained from FDTD simulations (solid lines).